frontiers in Physics

ORIGINAL RESEARCH
published: 27 September 2021
doi: 10.3389/fphy.2021.745075

Influence of the Weakening Effect of Drilling Fluid on Wellbore Stability in Anisotropic Shale Formation

Fan Zhang[1,2], Hou-Bin Liu[3], Shuai Cui[3], Ying-Feng Meng[3] and Jia-Jun Wang[3]*

[1]College of Petroleum Engineering, Xi'an Shiyou University, Xi'an, China, [2]Xi'an Shiyou University Shaanxi Key Laboratory of Well Stability and Fluid and Rock Mechanics in Oil and Gas Reservoirs, Xi'an, China, [3]State Key Laboratory of Oil and Gas Reservoir Geology and Exploitation, Southwest Petroleum University, Chengdu, China

For horizontal wells in Longmaxi Formation, oil-based drilling fluid that soaks for a long time is more likely to cause a wellbore collapse. Therefore, in this paper, the downhole core method of shale formation, in Longmaxi Formation, was adopted. First, rock samples were selected from different sampling angles and soaked with field drilling fluid. Second, a triaxial mechanics experiment was carried out. Based on the anisotropic wellbore stress distribution model, the stability of shale wellbore was calculated and analyzed. The results show that the compressive strength and cohesion of the shale are reduced after soaking in the drilling fluid. Hence, the reduction range of various sampling angles obviously differs as well. Shear failure occurs in vertical stratification; shear slip failure occurs along the weak plane, showing strong anisotropy. Combined with the experimental results, the collapse pressure is calculated, and it is found that the weakening effect of drilling fluid makes the overall collapse pressure rise by about 0.2 g/cm^3. Finally, the shale bedding dip and dip direction have a great influence on the collapse pressure. The lower critical mud weight always takes the minimum value when the borehole axis is perpendicular to the bedding.

Keywords: shale gas, anisotropy characterization method, weak bedding planes, collapse pressure, strength weakening

OPEN ACCESS

Edited by:
Qingxiang Meng,
Hohai University, China

Reviewed by:
Yue Li,
Sinosteel Maanshan General institute of Mining Research Co.Ltd, China
Shiyue Zhang,
Shanghai Research Institute of Materials, China

****Correspondence:***
Fan Zhang
fanz@xsyu.edu.cn

Specialty section:
This article was submitted to Interdisciplinary Physics, a section of the journal Frontiers in Physics

Received: *21 July 2021*
Accepted: *06 September 2021*
Published: *27 September 2021*

Citation:
Zhang F, Liu H-B, Cui S, Meng Y-F and Wang J-J (2021) Influence of the Weakening Effect of Drilling Fluid on Wellbore Stability in Anisotropic Shale Formation. Front. Phys. 9:745075. doi: 10.3389/fphy.2021.745075

INTRODUCTION

Shale accounts for more than 75% of the oil and gas deposits drilled globally [1]. The Longmaxi Formation, in Sichuan Basin, is rich in unconventional oil and gas resources. Moreover, the efficient development of shale gas holds great significance for prolonging the life of the petroleum industry in China [2]. The commercial development of Fuling shale gas, specifically, marks the rapid development of shale gas in China. At present, horizontal well drilling technology, and large-scale hydraulic fracturing, are key technologies for the successful development of shale gas. However, shale gas reservoirs are characterized by strong structural stress, strong formation heterogeneity and strong bedding development. However, irregular wellbore collapses and accidents often occur in drilling operations [3]. Considering the JY1HF well in the Jiaoshiba block area, for example, a wellbore collapse frequently occurred in the drilling process. The logging data showed that the wall expansion rate of the inclined section was as high as 50–100%. Therefore, an accurate understanding of the collapse rule, for the Longmaxi shale formation in Jiaoshiba, and the selection of the most optimal drilling design both have a significant influence on the efficient development of shale gas.

As for the collapse and instability of shale formation, scholars both at home and abroad have carried out a large number of studies from different perspectives. In the past, most of the studies focused on the

influence of the anisotropy characteristics of shale formation, specifically on its strength and its seepage characteristics. Among these studies, a series of mechanical experiments on different stratified shale were carried out [4–8], and some theoretical studies on heterogeneous rocks were also carried out [9–11]. It is recognized that the mechanical parameters (cohesion and angle of internal friction) of the bedding plane are the most important causes of shale failure [12]. It is also recognized that the seepage effect of the shale formation causes shale hydration, which has a significant impact on shale strength, and results in the reduction of cohesion and internal friction angle [13–15]. Wall rock strength decreases after prolonged exposure to drilling fluid [16–18]. A hydration test was conducted on the shale formation of Longmaxi, and it was discovered that the rock sample expanded with water absorption, permeated along the bedding, and finally peeled off the block [19]. Since another researcher established the wellbore stress distribution model based on anisotropy, and studied the wellbore instability, the anisotropy characteristics have become the focused research direction of the wellbore stability model [20]. Another researcher established a weak plane model and discovered that it is effective in predicting stratigraphic wellbore failure, except for obvious loose or plastic formations [21]. Therefore, it is determined that the direction of the weak plane is closely related to wellbore failure [22]. As a result, the isotropic wellbore stress distribution model is established [23, 24], and it is found that Poisson's ratio has little influence on borehole stability in shale formation [25, 26]. However, these studies often adopt assumed values, or only give experimental results, for the anisotropy of shale strength. Most of the research and literature adopts outcrop samples for the study of shale strength characteristics; few of them use the downhole core method of shale, and few of them use field drilling fluid to weaken it. In addition, the mechanical characteristics of the system are studied. Most shale hydration tests only use common formation water, or water-based drilling fluid, and there are few studies on the effect of oil-based drilling fluid on borehole wall instability.

In this paper, 2,450 m of downhole core from the Longmaxi Formation was adopted for the preparation of core from different sampling angles. Field oil-based drilling fluids were used to weaken the core in groups. Triaxial mechanical experiments were conducted on the core to obtain the mechanical parameters, before and after weakening of drilling fluids from different bedding angles. Next, combined with the single weak surface criterion and anisotropic wellbore stress distribution model, the calculation method of shale formation collapse pressure is established. Finally, mechanical parameters, before and after weakening, were used to study the variation law of collapse pressure in shale formations with different bedding occurrences. The results of this study can provide some theory and basis for guaranteeing borehole wall stability during drilling in the Longmaxi Formation.

Experiment and Analysis

There is a great deal of low-dip bedding in the shale formation of Jiaoshiba, and the strength of the shale formation is significantly reduced by the weak bedding surface, which shows obvious strength anisotropy. Meanwhile, Longmaxi shale is easy to hydrate [19], and oil-based drilling fluid is typically used for drilling in the field. However, long-term immersion of drilling fluid tends to reduce the shale strength. In order to better understand the influence of oil-base drilling fluid on the strength of shale with different drilling angles, the underground core of the Longmaxi Formation was used to carry out a triaxial mechanics experiment. Furthermore, the strength of shale at different angles, before and after drilling fluid immersion, were tested in order to provide parameters for the study of borehole wall stability in shale formation.

In order to study the rock mechanics parameters of bedding shale formation, only three bedding angles were taken, due to the difficulty in obtaining underground core. According to GB 23561.1-2009 "Determination of Physical Properties of Coal and Rock", the rock samples were made into specimens with a length and diameter of 50 mm × 25 mm where the included angle between the coring direction and the normal direction of the bedding surface of (a), was 90°, the included angle of (b) was 60°, and the included angle of (c) is 0° (as shown in **Figure 1**). All samples were dried in an oven at 60°C for 24 h and then set aside.

After drilling the core, the end face should be ground with a grinding machine, and the parallelism error of the two end faces should not exceed 0.5 mm. After the sample preparation, the triaxial mechanics experiment was carried out using a GCTS RTR-1000 (high temperature and high pressure) triaxial mechanics test machine. During the test, when the deformation rate signal feedback by the rock specimen was inconsistent with the predetermined signal, the servo controller would generate a corresponding comparison signal. This signal pushed the servo valve to move and increase or decrease the oil supply quantity of the loading device. Furthermore, the deformation rate of rock specimens was always controlled within an appropriate range. At the moment the rock specimen ruptured, its bearing capacity decreased, and its deformation rate increased. Then, the servo controller would actively close the servo valve, reduce the supply of oil source, and play the role of "letting pressure", so that the rock specimen could overcome the "burst" phenomenon. Next, the deformation data, after the peak value and before the peak value, can be obtained. Finally, the stress and strain data can be obtained in the process of rock deformation and failure under the formation conditions. In this experiment, each sampling angle was required to carry out experiments under two different confining pressures. The experimental loading confining pressures were 0 and 25 Mpa. The core was taken from the JY1HF well with vertical depth of 2450 m, so the confining pressure was set as 25MPa, and the confining pressure of 0 MPa was selected as the comparison. All cores were divided into two groups, A and B. Group A were dry cores, and Group B were immersed in an on-site oil-base drilling fluid for 30 days to simulate the downhole environment. It was found that in Group A, the compressive strength of the samples is the lowest when the included angle is 60°, and the strength of the samples in the vertical stratification direction is the highest (as shown in **Table 1**). The rock samples are shown in **Figure 2**. In addition, the damaged samples are shown in **Figure 3**. It was found that shear failure occurs at an angle of 0°, shear slip failure along the bedding plane occurs at an angle of 60°, and longitudinal cleavage failure occurs at an angle of 90°. Therefore, the shear slip failure along the weak bedding plane is the key failure mechanism that leads to the low strength of the bedding shale.

In addition, the cores of Group B were soaked with on-site, oil-base drilling fluid for 30 days, and subjected to triaxial

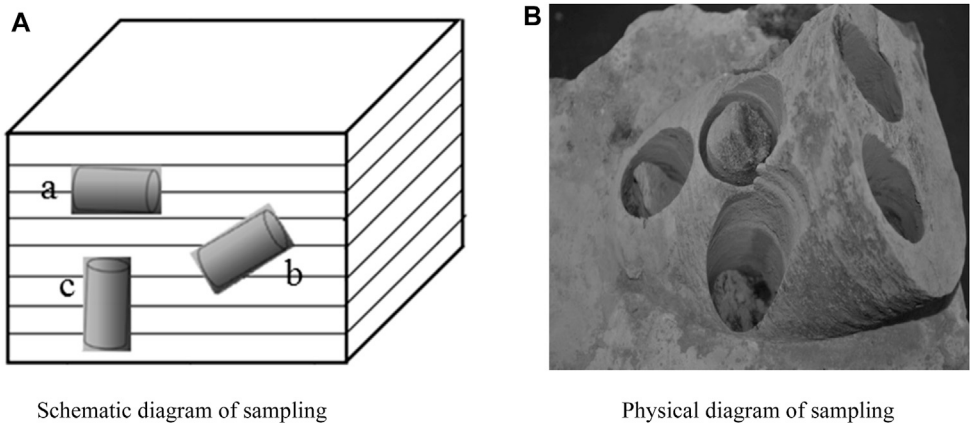

FIGURE 1 | Sampling diagram at different bedding angles.

TABLE 1 | Triaxial test results of dry samples of Group A.

Test number	Sampling angle (°)	Category	Experimental confining pressure (MPa)	Poisson's ratio (-)	Elastic modulus (MPa)	Compressive strength (MPa)	Cohesion (MPa)	Angle of internal friction (°)
A-0-1	0	dry	0	0.191	24,527.0	169.7	56.14	23.02
A-0-2		dry	25	0.231	24,143.6	226.8		
A-60-1	60	dry	0	0.117	7,048.3	45.5	20.17	6.88
A-60-2		dry	25	0.154	18,747.4	77.3		
A-90-1	90	dry	0	0.155	25,274.2	129.7	38.00	29.26
A-90-2		dry	25	0.202	22,095.8	202.5		

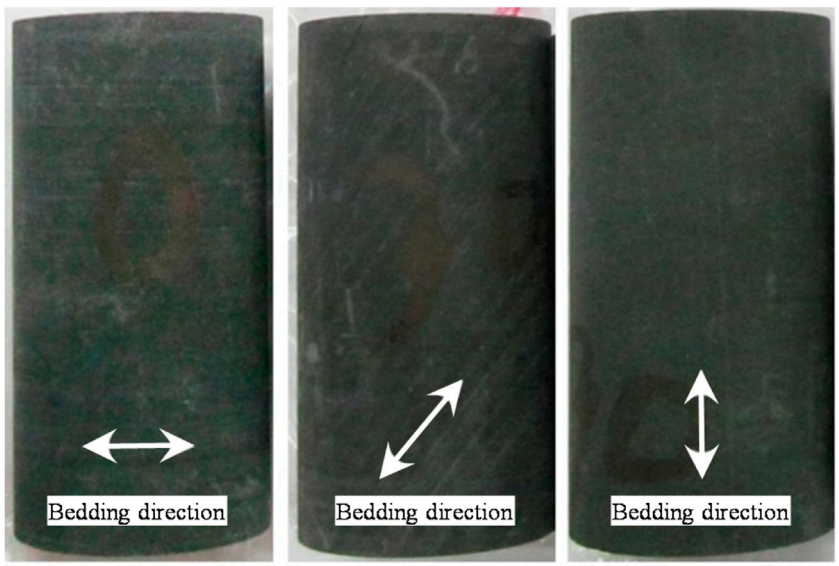

FIGURE 2 | Rock samples before failure of triaxial rock mechanics test.

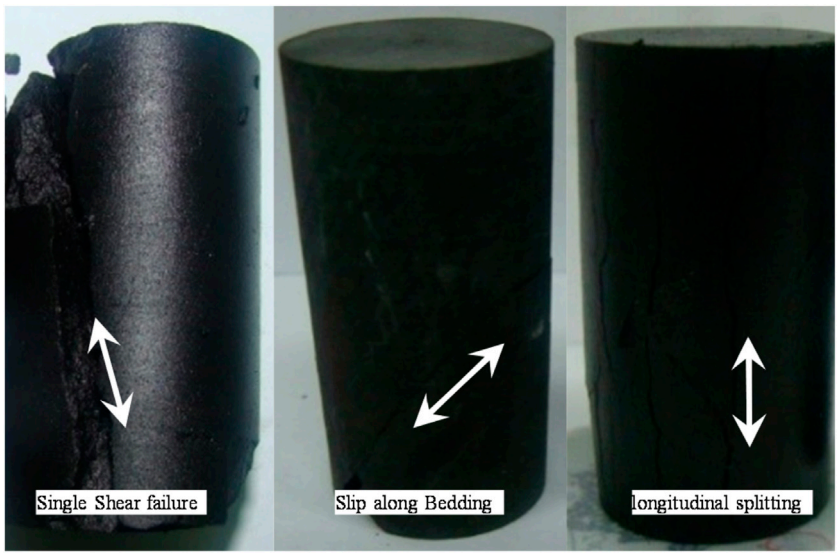

FIGURE 3 | Rock samples after failure of triaxial rock mechanics test.

TABLE 2 | Triaxial test results of soaked samples of Group B.

Test number	Sampling angle (°)	Category	Experimental confining pressure (MPa)	Poisson's ratio (-)	Elastic modulus (MPa)	Compressive strength (MPa)	Cohesion (MPa)	Angle of internal friction (°)
B-0-1	0	soak	0	0.150	19,945.7	134.2	47.26	19.69
B-0-2		soak	25	0.283	25,554.7	184.6		
B-60-1	60	soak	0	0.228	9,732.7	30.8	14.15	4.83
B-60-2		soak	25	0.106	31,862.8	60.4		
B-90-1	90	soak	0	0.276	16,192.3	70.2	20.26	30.00
B-90-2		soak	25	0.213	33,643.3	145.2		

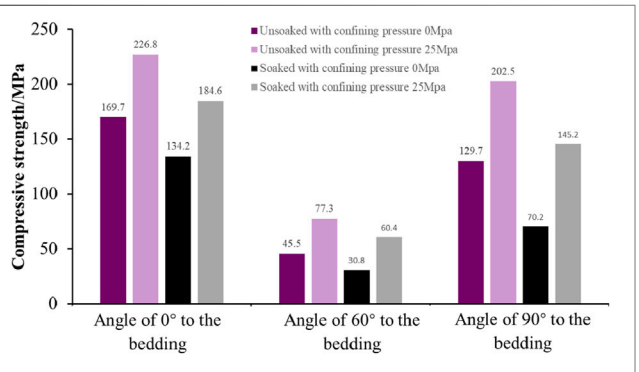

FIGURE 4 | Comparison of compressive strength before and after drilling fluid immersion.

mechanical experiments. The experimental results are shown in **Table 2**.

The results of three-axis experiments of shale, before and after soaking, are compared (as shown in **Figure 4** and **Figure 5**). It is found that the cohesion and internal friction angle of the shale matrix and bedding decreased when soaking time was increased. **Figure 4** shows that after drilling fluid immersion, the compressive strength of shale with different sampling angles decreases at 0 and 25 MPa confining pressure. Among them, at the angles of 0° and 90°, the compressive strength decreases greatly, while at the angle of 60°, the compressive strength only slightly decreases. Because the strength of the rock sample is very low at an angle of 60°, the space for decline is very limited. **Figure 5** shows that the shale cohesion and internal friction angle of different sampling angles decrease after immersion in drilling fluid, and cohesion decreases the most when the angle is 90°. Moreover, the compressive strength of some rock samples increases after immersion, which may be due to heterogeneity. The influence of oil-based drilling fluid on shale strength may be one of the key factors of wellbore instability. Therefore, the data fitting of shale strength before and after soaking was carried out (as shown in **Figure 6**). The fitting correlation coefficient is close to 1, and the fitting regression effect is good. The compressive strength of shale in Jiaoshiba area from different angles can be predicted according to the fitting formula.

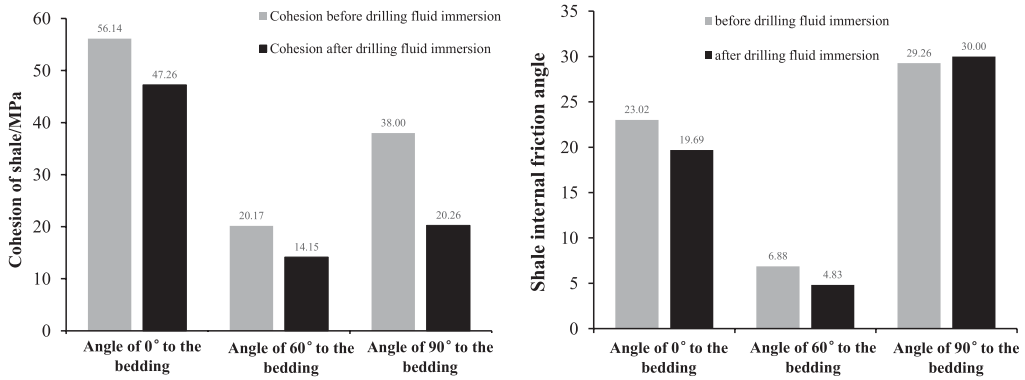

FIGURE 5 | Cohesion and angle of internal friction before and after immersion.

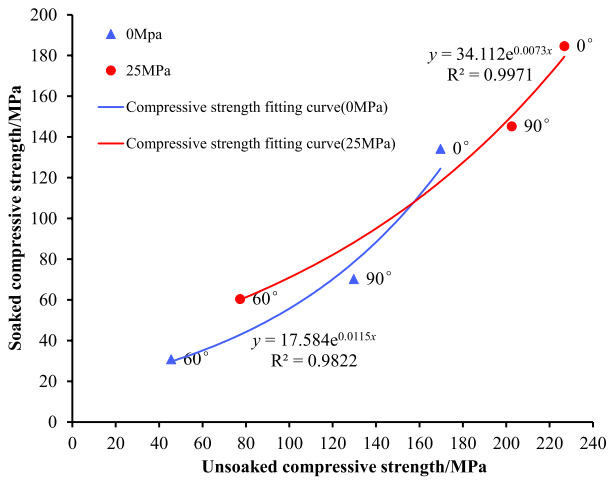

FIGURE 6 | Fitting of compressive strength data before and after immersion.

Wellbore Stability Analysis Model and Criterion of Anisotropic Formation

It is necessary to establish a wellbore stability analysis model for the anisotropic formation of shale after triaxial mechanics experiments, with different included angles, are performed. Then, combined with the rock failure criterion, the influence of drilling fluid weakening on the stability of shale formation wellbore can be estimated.

Wellbore Stabilization Model for Anisotropic Formation

Assuming the formation is completely heterogeneous, and on the basis of only considering the elastic deformation of the material line, according to the generalized Hooke's law the stiffness matrix contains 21 elastic constants. Because the Longmaxi Formation belongs to bedding strata, the bedding strata can be equated with transverse isotropic materials. At this point, the flexibility matrix can be simplified, including five independent flexibility coefficients, and the constitutive equation can be expressed as **Eq. 1**:

$$\begin{bmatrix} \varepsilon_x \\ \varepsilon_y \\ \varepsilon_z \\ \gamma_{yz} \\ \gamma_{zx} \\ \gamma_{xy} \end{bmatrix} = \begin{bmatrix} S_{11} & S_{12} & S_{13} & & & \\ S_{21} & S_{22} & S_{23} & & & \\ S_{31} & S_{32} & S_{33} & & & \\ & & & S_{44} & & \\ & & & & S_{55} & \\ & & & & & S_{66} \end{bmatrix} \begin{bmatrix} \sigma_x \\ \sigma_y \\ \sigma_z \\ \tau_{yz} \\ \tau_{zx} \\ \tau_{xy} \end{bmatrix} \tag{1}$$

Among them, the parameter is specific, as expressed in **Eq. 2**:

$$\begin{cases} S_{11} = S_{22} = 1/E_h \\ S_{12} = S_{21} = -\nu_h/E_h \\ S_{13} = S_{31} = S_{23} = S_{32} = -\nu_v/E_v \\ S_{33} = 1/E_v \\ S_{44} = S_{55} = 1/E_h + 1/E_v + 2\nu_v/E_h \\ S_{66} = 2(1+\nu_h)/E_h \end{cases} \tag{2}$$

Under the bedding plane coordinate system, the rock equilibrium equation and the strain coordination equation are represented in **Eq. 3** and **Eq. 4**, respectively, according to the assumed conditions, when the rock around the well meets the plane strain assumption.

$$\begin{cases} \dfrac{\partial \sigma_x}{\partial x} + \dfrac{\partial \tau_{yx}}{\partial y} = 0 \\ \dfrac{\partial \sigma_{yx}}{\partial x} + \dfrac{\partial \sigma_y}{\partial y} = 0 \\ \dfrac{\partial \tau_{zx}}{\partial x} + \dfrac{\partial \tau_{zy}}{\partial y} = 0 \end{cases} \tag{3}$$

$$\begin{cases} \dfrac{\partial^2 \varepsilon_x}{\partial y^2} + \dfrac{\partial^2 \varepsilon_y}{\partial x^2} = \dfrac{\partial^2 \gamma_{xy}}{\partial x \partial y} \\ \dfrac{\partial \gamma_{zx}}{\partial y} - \dfrac{\partial \gamma_{yz}}{\partial x} = 0 \\ \dfrac{\partial^2 \varepsilon_z}{\partial y^2} = \dfrac{\partial^2 \varepsilon_z}{\partial x^2} = \dfrac{\partial^2 \varepsilon_z}{\partial x \partial y} \end{cases} \tag{4}$$

In order to solve the problems listed, the stress function $F(x, y)$ and $\Psi(x, y)$ is introduced, so that each stress in the balance equation can be expressed as **Eq. 5**:

$$\sigma_x = \frac{\partial^2 F}{\partial y^2}, \sigma_y = \frac{\partial^2 F}{\partial x^2}, \tau_{xy} = -\frac{\partial^2 F}{\partial x \partial y}, \tau_{xz} = -\frac{\partial \Psi}{\partial y}, \tau_{yz} = -\frac{\partial \Psi}{\partial x} \quad (5)$$

Since it is a plane strain problem, it can be obtained from the physical equation. The axial stress σ_z can be solved by **Eq. 6**, as follows:

$$\sigma_z = -\frac{1}{S_{33}}\left(S_{31}\sigma_x + S_{32}\sigma_y + S_{34}\tau_{yz} + S_{35}\tau_{zx} + S_{36}\tau_{xy}\right) \quad (6)$$

For the exact solution of stress concentration in anisotropic rock, two stress functions about stress components are defined, and the general expressions of stress function are given, as shown in **Eq. 7**:

$$\begin{cases} F = 2\mathrm{Re}[F_1(z_1) + F_2(z_2) + F_3(z_3)] \\ \Psi = 2\mathrm{Re}\left[\lambda_1 F_1'(z_1) + \lambda_2 F_2'(z_2) + \dfrac{F_3'(z_3)}{\lambda_3}\right] \end{cases} \quad (7)$$

Setiawan [23] introduced a new complex variable function on complex variables, which was expressed as **Eq. 8**:

$$\phi_1(z_1) = F_1'(z_1), \phi_2(z_2) = F_2'(z_2), \phi_3(z_3) = \frac{1}{\lambda_3}F_3'(z_3) \quad (8)$$

By using the above formula, **Eq. 9** of the stress component in bedding wells is given:

$$\begin{cases} \sigma_{x,h} = 2\mathrm{Re}\left[\mu_1^2\phi_1'(z_1) + \mu_2^2\phi_2'(z_2) + \mu_3^2\lambda_3\phi_3'(z_3)\right] \\ \sigma_{y,h} = 2\mathrm{Re}\left[\phi_1'(z_1) + \phi_2'(z_2) + \lambda_3\phi_3'(z_3)\right] \\ \tau_{xy,h} = -2\mathrm{Re}\left[\mu_1\phi_1'(z_1) + \mu_2^2\phi_2'(z_2) + \mu_3^2\lambda_3\phi_3'(z_3)\right] \\ \tau_{xz,h} = 2\mathrm{Re}\left[\lambda_1\mu_1\phi_1'(z_1) + \lambda_2\mu_2\phi_2'(z_2) + \mu_3\lambda_3\phi_3'(z_3)\right] \\ \tau_{yz,h} = -2\mathrm{Re}\left[\lambda_1\phi_1'(z_1) + \lambda_2\phi_2'(z_2) + \phi_3'(z_3)\right] \\ \sigma_{z,h} = -\dfrac{1}{S_{33}}\left(S_{31}\sigma_x + S_{32}\sigma_y + S_{34}\tau_{yz} + S_{35}\tau_{zx} + S_{36}\tau_{xy}\right) \end{cases} \quad (9)$$

Finally, the formula of stress components around borehole is expressed in **Eq. 10**.

$$\begin{cases} \sigma_x' = \sigma_{xx} + 2\mathrm{Re}\left[\mu_1^2\phi_1'(z_1) + \mu_2^2\phi_2'(z_2) + \mu_3^2\lambda_3\phi_3'(z_3)\right] \\ \sigma_y' = \sigma_{yy} + 2\mathrm{Re}\left[\phi_1'(z_1) + \phi_2'(z_2) + \lambda_3\phi_3'(z_3)\right] \\ \tau_{xy}' = \tau_{xy} - 2\mathrm{Re}\left[\mu_1\phi_1'(z_1) + \mu_2^2\phi_2'(z_2) + \mu_3^2\lambda_3\phi_3'(z_3)\right] \\ \tau_{xz}' = \tau_{xz} + 2\mathrm{Re}\left[\lambda_1\mu_1\phi_1'(z_1) + \lambda_2\mu_2\phi_2'(z_2) + \mu_3\lambda_3\phi_3'(z_3)\right] \\ \tau_{yz}' = \tau_{yz} - 2\mathrm{Re}\left[\lambda_1\phi_1'(z_1) + \lambda_2\phi_2'(z_2) + \phi_3'(z_3)\right] \\ \sigma_z' = \sigma_{xx} - \dfrac{1}{S_{33}}\left(S_{31}\sigma_x + S_{32}\sigma_y + S_{34}\tau_{yz} + S_{35}\tau_{zx} + S_{36}\tau_{xy}\right) \end{cases} \quad (10)$$

The borehole stability model, **Eq. 11**, under polar coordinates, can be obtained by plugging into the borehole polar coordinate formula:

$$\begin{cases} \sigma_r = \frac{\sigma_x' + \sigma_y'}{2}\left(1 - \frac{r_i^2}{r^2}\right) + \frac{\sigma_x' - \sigma_y'}{2}\left(1 - 4\frac{r_i^2}{r^2} + 3\frac{r_i^4}{r^4}\right)\cos 2\theta + \tau_{xy}'\left(1 + 3\frac{r_i^4}{r^4} - 4\frac{r_i^2}{r^2}\right)\sin 2\theta + \frac{r_i^2}{r^2}p_w - \alpha p_p \\ \sigma_\theta = \frac{\sigma_x' + \sigma_y'}{2}\left(1 + \frac{r_i^2}{r^2}\right) - \frac{\sigma_x' - \sigma_y'}{2}\left(1 + 3\frac{r_i^4}{r^4}\right)\cos 2\theta - \tau_{xy}'\left(1 + 3\frac{r_i^4}{r^4} - 4\frac{r_i^2}{r^2}\right)\sin 2\theta - \frac{r_i^2}{r^2}p_w - \alpha p_p \\ \sigma_z = \sigma_z' + \mu\left[\sigma_x' + \sigma_y' - 2\left(\sigma_x' - \sigma_y'\right)\frac{r_i^2}{r^2}\cos 2\theta + 4\tau_{xy}'\sin 2\theta\right] - \alpha p_p \\ \tau_{r\theta} = \tau_{xy}'\left(1 + 3\frac{r_i^4}{r^4} - 4\frac{r_i^2}{r^2}\right)\cos 2\theta \\ \tau_{\theta z} = \tau_{yz}'\left(1 + \frac{r_i^2}{r^2}\right)\cos\theta - \tau_{xz}'\left(1 + \frac{r_i^2}{r^2}\right)\sin\theta \\ \tau_{rz} = \tau_{xz}'\left(1 - \frac{r_i^2}{r^2}\right)\cos\theta + \tau_{yz}'\left(1 - \frac{r_i^2}{r^2}\right)\sin\theta \end{cases} \quad (11)$$

where, $\sigma_r, \sigma_\theta, \sigma_z, \tau_{r\theta}, \tau_{\theta z}$ and τ_{rz} is the stress component under the borehole column coordinates; r_i is the borehole radius; r is the radial distance between surrounding rocks and borehole axis; μ is the Poisson's ratio of rock; and θ is the well circumference angle. According to the formula listed above, the stress distribution of the surrounding rock, under the coordinates of any inclined shaft, can be obtained when the original ground stress and the liquid column pressure in the wellbore are acted upon.

Shale Matrix Failure Criteria

It is necessary to select appropriate strength criterion for accurately evaluating the stratigraphic stability. According to the test results, when the included angle of the rock sample is 0°, the rock is considered a single shear failure. Rock failure shear force on the shear surface must overcome rock cohesion and friction, as shown in **Eq. 12**:

$$\tau = c + \sigma\tan\varphi \quad (12)$$

M-C criterion can be expressed as **Eq. 13** in the form of principal stress, as shown in **Figure 7**.

$$\sigma_1 = \sigma_3\cot^2\left(45^0 - \frac{\varphi}{2}\right) + 2c\cot\left(45^0 - \frac{\varphi}{2}\right) \quad (13)$$

Strength Criterion for Weak Plane

According to the test results, when the included angle of the sample is 60°, the sample is shear-slippage failure along the bedding plane. The local layer slips along the weak surface, and it is unstable when the surrounding rock is destroyed by the crack structure surface. For a formation containing micro-fractures, when the angle between the fracture surface and the maximum principal stress is within a certain range [21], the formation will appear to collapse, and drop blocks along the fracture surface. Strength criterion is expressed as **Eq. 14**:

$$\sigma_\theta - \sigma_r = \frac{2\left(c_w + \tan\varphi_w \cdot \left(\sigma_r - \alpha \cdot p_p\right)\right)}{\left(1 - \tan\varphi_w\cot\beta\right)\sin 2\beta} \quad (14)$$

where σ_θ is the circumferential stress on borehole, Pa; σ_r is radial stress, Pa; α is Biot coefficient; P_P is pore pressure, Pa; c_w is cohesion of shale bedding, Pa; φ_w is friction angle of shale bedding, °; and β is the angle between weak-plane normal and maximum principal stress, °. However, the weak plane criterion needs to satisfy **Eq. 15** in order to make the rock sample shear slip along the weak plane, as shown in **Figure 8**.

$$\sigma_1 = \sigma_3 \cot^2\left(45^0 - \frac{\varphi}{2}\right) + 2c\cot\left(45^0 - \frac{\varphi}{2}\right)$$

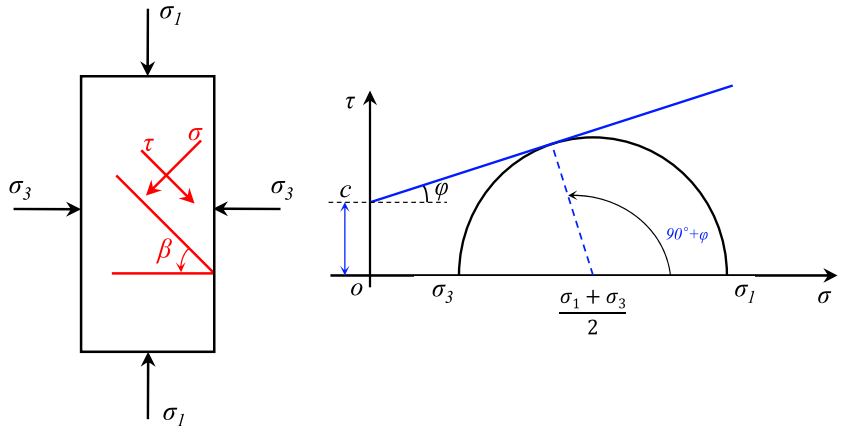

FIGURE 7 | Failure mode and M-C circle for single shear failure.

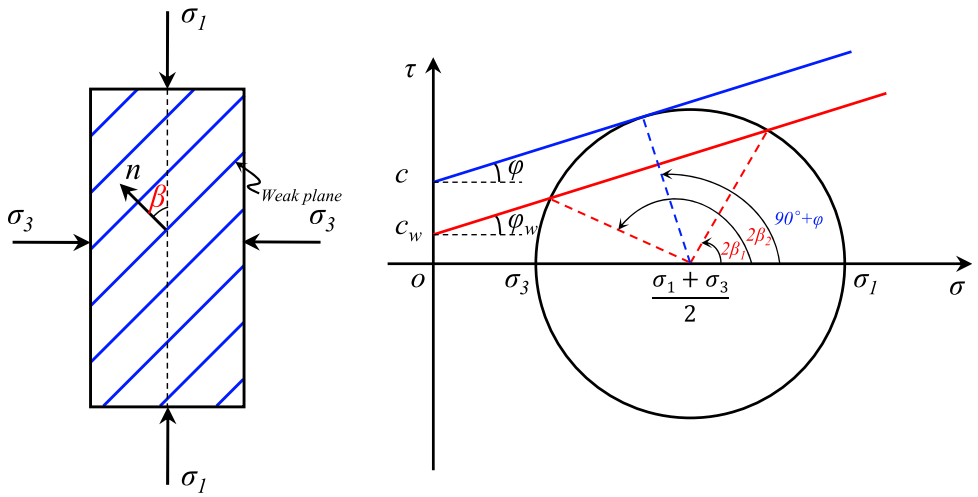

FIGURE 8 | Failure mode under the single weak plane criterion.

$$\begin{cases} \beta_1 = \dfrac{\varphi_w}{2} + \dfrac{1}{2}\arcsin\left[\dfrac{(\sigma_1 + \sigma_3 + 2c_w\cot\varphi_w)\sin\varphi_w}{\sigma_1 - \sigma_3}\right] \\ \beta_2 = \dfrac{\pi}{2} + \dfrac{\varphi_w}{2} - \dfrac{1}{2}\arcsin\left[\dfrac{(\sigma_1 + \sigma_3 + 2c_w\cot\varphi_w)\sin\varphi_w}{\sigma_1 - \sigma_3}\right] \\ 2\beta_1 \le 2\beta \le 2\beta_2 \end{cases} \quad (15)$$

INFLUENCE OF DRILLING FLUID ON WELLBORE STABILITY OF BEDDED SHALE

In this paper, polar coordinates are used to characterize the minimum drilling fluid density in the shale formation of the Longmaxi Formation with the change of drilling direction, and the influence of weak surface. Based on the experimental data, the variation rule of formation collapse pressure is compared and analyzed before and after drilling fluid weakening.

Geomechanics Parameters and Rock Mechanical Parameters

In this model, the X axis is consistent with the north geographical pole, and the Y axis is aligned with the east geographical pole. Weak plane occurrence is defined by inclination direction (α) and inclination angle (β). In order for the weak plane to be studied in the wellbore stability analysis model, the inclination angle is assumed to be 30° and 60°, and the study is carried out under different inclinations. The experimental samples, in this paper, are the underground core of Longmaxi Formation, with a

TABLE 3 | Geomechanical parameters of Longmaxi Formation in Fuling.

No	Parameters	Value	unit
1	Depth	2,450	m
2	Maximum horizontal *in situ* stress	2.8	MPa/100m
3	Minimum horizontal *in situ* stress	2.21	MPa/100m
4	Vertical *in situ* stress	2.61	MPa/100m
5	Pore pressure	1.15	MPa/100m
6	Biot coefficient	0.45	—

sampling depth of 2,450 m. According to the field hydraulic fracturing and logging data, the geomechanics parameters of the target interval were obtained (as shown in **Table 3**). Then, according to laboratory rock mechanics experiments, rock mechanics parameters, before and after drilling fluid immersion, are obtained (as shown in **Table 4**). All these parameters are input parameters for the lower critical mud weight analysis of the Longmaxi shale formation in Fuling.

Collapse Pressure of Rational Formation Before and After Drilling Fluid Immersion

In shale formations, horizontal wells usually pass through bedding strata with different well angles, and bedding strata also have different tendencies, which affects the formation's lower critical mud weight, and the choice of the optimal drilling direction. In addition, it is found that bedding inclination angles are mostly low-dip angles in field drilling construction. Therefore, the formation dip angle of 30° and 60° were selected for the study. Based on the experimental data, the influence of drilling fluid on wellbore stability of shale formation is studied. The purpose is to get closer to identifying the best working conditions, and also choose the optimal drilling construction scheme.

When the bedding inclination angle is 30°, it is found that the collapse pressure is generally lower along the direction of bedding tendency, or its relative direction (as shown in **Figure 9**). However, in the direction where the angle with bedding tendency is 90°, the collapse pressure is generally heightened to the maximum value, which is not suitable for a drilling well trajectory direction. Moreover, with the increase of the azimuth of stratigraphic tendency, the lower critical mud weight of bedding tendency decreases gradually, with a decrease of 0.3 g/cm^3. In the direction of bedding inclination, the closer the angle of the well inclination is to the bedding inclination, the lower the collapse pressure. The collapse pressure is minimal when the axial direction of borehole is perpendicular to the bedding. Combined with the laboratory triaxial rock mechanics experiment, it is found that when the loading direction is perpendicular to the bedding, the maximum rock mechanical parameters are taken, so the borehole is more stable. By comparing and analyzing the collapse pressure, before and after drilling fluid immersion, the overall lower critical mud weight increased to a certain extent. The minimum collapse pressure rose to 0.2 g/cm^3, while the maximum collapse pressure rose from 1.75 g/cm^3 to 1.95 g/cm^3. However, the choice of borehole for the azimuth angle is greater than it was before immersion. Drilling is not necessary along the bedding tendency, but within a certain angle to the bedding tendency. The optimal drilling azimuth is changed to an angle of about 30° with the bedding tendency.

When the bedding inclination angle is 60°, the change of collapse pressure is shown in **Figure 10**. It is found that with the increase of the bedding inclination angle, the figure shows that different bedding plane inclination angles have a significant effect on the collapse pressure density of the shaft wall. When the inclination is 0°, the included angle with the azimuth angle is 30°, which is the optimal drilling direction. The overall lower critical mud weight is around 1.45 g/cm^3. When the angle of inclination is 30° and the well bevel is below 40°, the collapse pressure is higher than 1.70 g/cm^3. When the inclination angle is 60°, the optional orientation of the wellbore trajectory is smaller, and the collapse pressure is lower, but only when the well is drilled with a high inclination angle in the bedding inclination azimuth. Also, the minimum collapse pressure is 1.1 g/cm^3. When the inclination angle is 90°, the lower critical mud weight is smaller, in the range of about 30° of bedding tendency, and the collapse pressure range is 1.1–1.4 g/cm^3. The collapse pressure, before and after soaking, is compared and analyzed. Similar to the inclination angle with bedding of 30°, the overall rise amplitude of the collapse pressure is 0.2 g/cm^3. However, the choice of borehole orientation is larger, and the collapse pressure is higher, but only in a small range. When the trend is 0°, the larger value is 1.9 g/cm^3 when the azimuth angle is 60°. When the trend is 30°, the collapse pressure is higher than 1.9 g/cm^3, within the azimuth range of 0°–60° and 210°–240°. When the trend is 60°, the value of collapse pressure is higher, in the azimuth range of 90°–180° and 270°–360°. When the trend is 90°, the optimal drilling direction is 60°–120° and 240°–300°, and the collapse pressure is lower than 1.6 g/cm^3.

TABLE 4 | Mechanical parameters of rock before and after immersion.

Parameters before immersion(A)	Value	Parameters after immersion(B)	Value
Cohesion of rock matrix (MPa)	56.14	Cohesion of rock matrix (MPa)	47.26
Friction angle of rock matrix (Deg)	23.02	Friction angle of rock matrix (Deg)	19.69
Cohesion of shale bedding (MPa)	20.17	Cohesion of shale bedding (MPa)	14.15
Friction angle of shale bedding (Deg)	6.88	Friction angle of shale bedding (Deg)	4.83
elastic modulus vertical with bedding plane (GPa)	24.14	elastic modulus vertical with bedding plane (GPa)	25.56
elastic modulus along with bedding plane (GPa)	18.75	elastic modulus along with bedding plane (GPa)	31.86
Poisson's ratio	0.195	Poisson's ratio	0.193

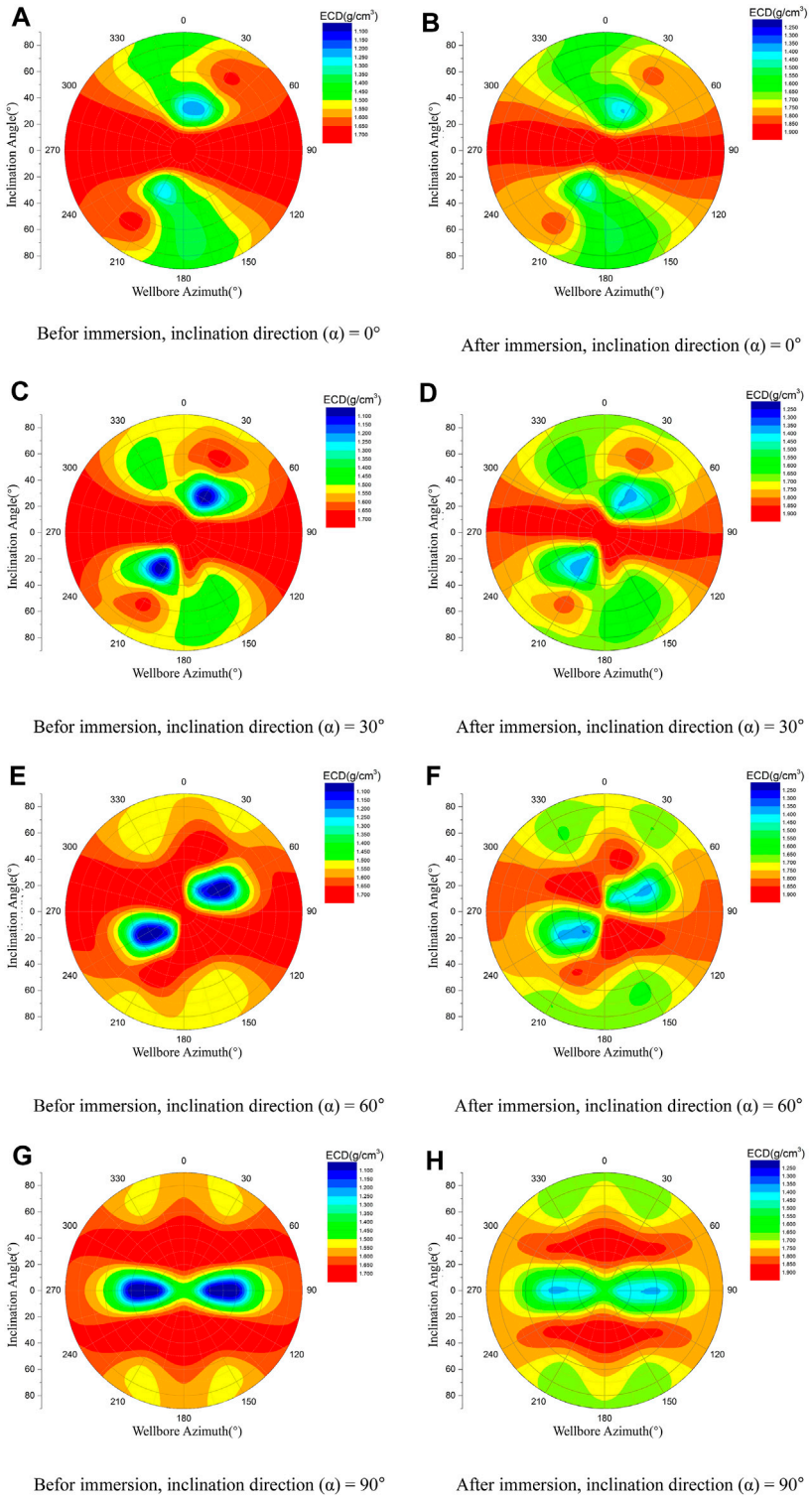

FIGURE 9 | The collapse pressure before and after soaking, when the bedding inclination angle (β) is 30°.

By comparing and analyzing the bedding inclination angles of 30° and 60°, with the increase of the bedding inclination angle, the optimal well inclination angle also increases. When the borehole axis is perpendicular to the bedding surface, the minimum value of lower critical mud weight is always set. In addition, when the bedding inclination angle is 30°, the optional borehole bearing

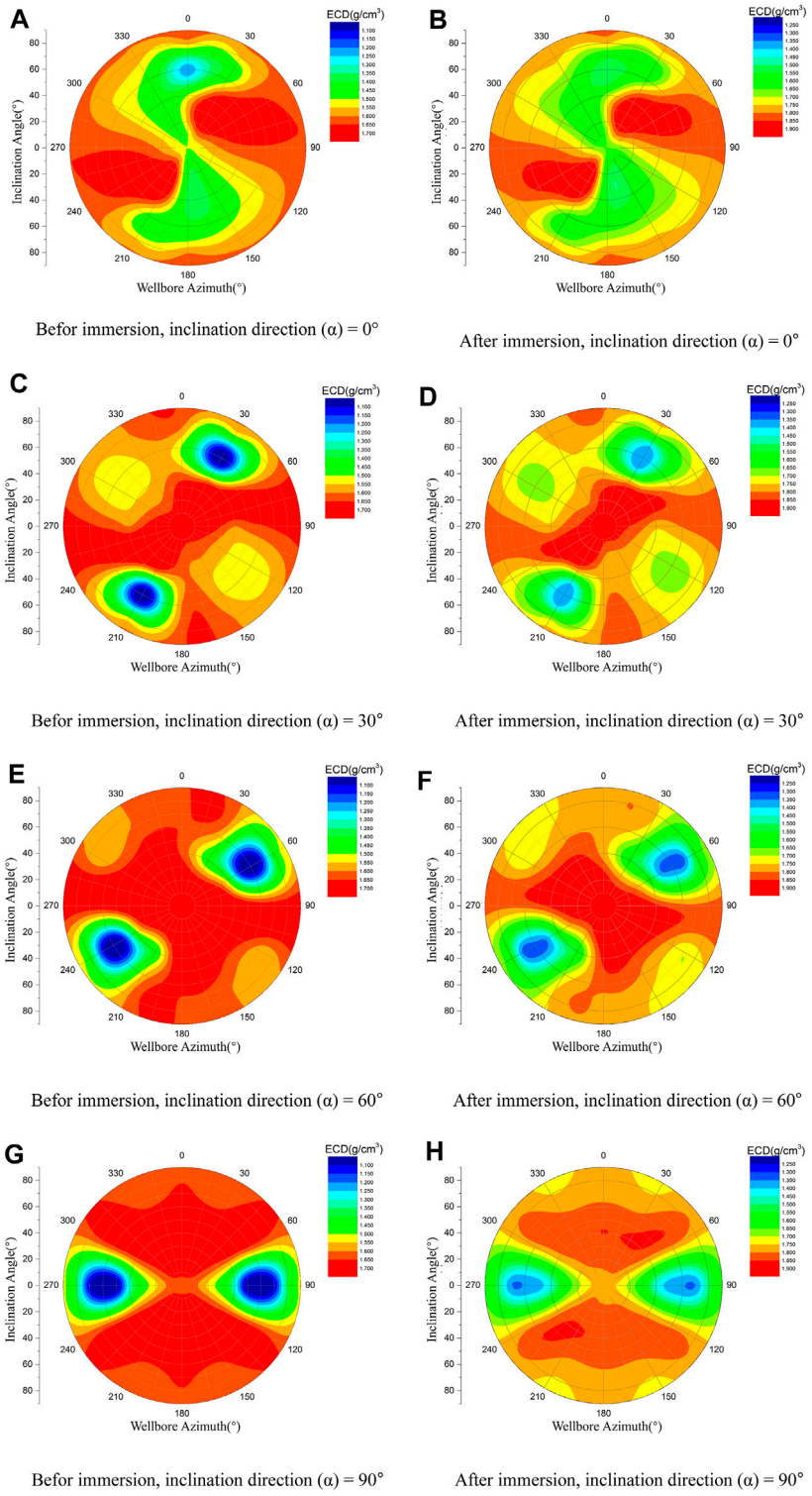

FIGURE 10 | The collapse pressure before and after soaking, when the bedding inclination angle(β) is 60°.

angle is also more concentrated than when the bedding inclination angle is 60°. When the bedding inclination angle is 60°, the collapse pressure changes are more complex, and the bedding occurrence has a significant influence on the selection of the optimal drilling direction. Finally, the oil-base drilling fluid has a significant effect on shale strength, making the overall

minimum drilling fluid density increase by about 0.2 g/cm^3, and the maximum collapse pressure rise from 1.75 g/cm^3 to 1.95 g/cm^3. In other words, the mechanism of shale mechanical failure, bedding occurrence and weakening effect of drilling fluid, are all very important in the wellbore stability analysis of shale formation.

CONCLUSION

In this paper, the triaxial mechanics experiments of different bedding angles and different confining pressure conditions are carried out by examining the shale of Longmaxi Formation in Fuling, for example. Based on the experimental data, the variation law of wellbore collapse pressure, before and after drilling fluid immersion, is studied. The main controlling factors of borehole collapse are revealed in the middle rational shale formation during drilling. The following conclusions are obtained:

1) Because of the shale bedding development of Longmaxi Formation, the strength of weak bedding is lower than that of shale body. The compressive strength of the specimens is the lowest under the condition of a 60° angle with bedding, and the cohesion and internal friction angle are also the lowest. However, the strength of the samples is the highest in the vertical stratification direction, and the cohesion and internal friction angle are also the highest. This indicates that Longmaxi shale shows strong intensity anisotropy.

2) Experimental results of triaxial rock mechanics show that the samples have shear failure in the vertical bedding direction. The samples specifically have shear slip failure along the bedding plane at an angle of 60° with the bedding plane, and the samples occur split failure in the parallel bedding direction. This indicates that shear slip failure along the weak bedding plane is the key mechanical mechanism that leads to the decrease of shale strength.

3) After soaking the drilling fluid, the compressive strength, cohesion, and angle of internal friction of the shale all have measured changes. The compressive strength decreases after soaking, in which the compressive strength decreases the most under 90°, and is very low before soaking under 60°, where the decrease is the smallest. The cohesion decreases after soaking, where the degree of decline was the highest at 90°, and the smallest at 60°. Meanwhile, the internal friction angle did not change obviously after immersion.

4) The bedding occurrence has a great influence on the distribution law of collapse pressure. When the borehole axis is perpendicular to the bedding surface, the minimum value of lower critical mud weight is always taken. While at a low bedding dip, the optimal drilling direction is more concentrated. As the azimuth of bedding tendency increases, the distribution of collapse pressure becomes more complicated.

5) The weakening effect of the drilling fluid makes the overall collapse pressure rise by about 0.2 g/cm^3. Before the drilling fluid weakens, the collapse pressure tends to take the minimum value on the bedding tendency. After weakening, the collapse pressure is distributed more evenly in the appropriate direction, and the included angle of 30°, with the bedding tendency, can also be the optimal direction.

DATA AVAILABILITY STATEMENT

The original contributions presented in the study are included in the article/**Supplementary Material**, further inquiries can be directed to the corresponding author.

AUTHOR CONTRIBUTIONS

Writing-original draft preparation, FZ; writing-review and editing, FZ and H-BL; methodology, Y-FM; software, FZ; data curation, SC and J-JW; All authors have read and agreed to the published version of the manuscript.

FUNDING

This research was financially supported by Open Fund of Shaanxi Key Laboratory of Advanced Stimulation Technology for Oil Gas Reservoirs, grant number 20JS120; Young science and Technology Talents Foundation of Shaanxi province, grant number 2019KJXX-054; National Natural Science Foundation of China, grant numbers (41702146, 51934005, 51874242).

SUPPLEMENTARY MATERIAL

The Supplementary Material for this article can be found online at: https://www.frontiersin.org/articles/10.3389/fphy.2021.745075/full#supplementary-material

REFERENCES

1. Duan K, and Kwok CY. Evolution of Stress-Induced Borehole Breakout in Inherently Anisotropic Rock: Insights from Discrete Element Modeling. *J Geophys Res Solid Earth* (2016) 121(4):2361–81. doi:10.1002/2015jb012676
2. Caineng ZOU, Guangming Z, Zhang G, Wang H, Zhang G, Li J, et al. Formation, Distribution, Potential and Prediction of Global Conventional and Unconventional Hydrocarbon Resources[J]. *Pet Exploration Develop* (2015) 42(1):14–28. doi:10.1016/s1876-3804(15)60002-7
3. Liang C, Chen M, Jin Y, and Lu Y. Wellbore Stability Model for Shale Gas Reservoir Considering the Coupling of Multi-Weakness Planes and Porous Flow. *J Nat Gas Sci Eng* (2014) 21:364–78. doi:10.1016/j.jngse.2014.08.025
4. Ma T, Peng N, Zhu Z, Zhang Q, Yang C, and Zhao J. Brazilian Tensile Strength of Anisotropic Rocks: Review and New Insights. *Energies* (2018) 11(2):304. doi:10.3390/en11020304
5. Guo W, Shen W, Li X, Wang N, Liu X, Zhang X, et al. Study on Mechanical Characteristics and Damage Mechanism of the Longmaxi Formation Shale in Southern Sichuan Basin, China. *Energy Exploration & Exploitation* (2020) 38(2):454–72. doi:10.1177/0144598719876858
6. Suo Y, Chen Z, Rahman SS, and Chen X. Experimental Study on Mechanical and Anisotropic Properties of Shale and Estimation of Uniaxial Compressive

Strength[J]. *Energy Sourc A: Recovery, Utilization, Environ Effects* (2020) 1–11. doi:10.1080/15567036.2020.1779873
7. Heng S, Li X, Liu X, and Chen Y. Experimental Study on the Mechanical Properties of Bedding Planes in Shale. *J Nat Gas Sci Eng* (2020) 76:103161. doi:10.1016/j.jngse.2020.103161
8. Zuo J, Lu J, Ghandriz R, Wang J, Li Y, Zhang X, et al. Mesoscale Fracture Behavior of Longmaxi Outcrop Shale with Different Bedding Angles: Experimental and Numerical Investigations[J]. *J Rock Mech Geotechnical Eng* (2020) 12(2):297–309. doi:10.1016/j.jrmge.2019.11.001
9. Meng Q-X, Wang H-L, Xu W-Y, and Chen Y-L. Numerical Homogenization Study on the Effects of Columnar Jointed Structure on the Mechanical Properties of Rock Mass. *Int J Rock Mech Mining Sci* (2019) 124:104127. doi:10.1016/j.ijrmms.2019.104127
10. Meng Q-X, Xu W-Y, Wang H-L, Zhuang X-Y, Xie W-C, and Rabczuk T. DigiSim - an Open Source Software Package for Heterogeneous Material Modeling Based on Digital Image Processing. *Adv Eng Softw* (2020) 148: 102836. doi:10.1016/j.advengsoft.2020.102836
11. Meng Q, Wang H, Cai M, Xu W, Zhuang X, and Rabczuk T. Three-dimensional Mesoscale Computational Modeling of Soil-Rock Mixtures with Concave Particles. *Eng Geology* (2020) 277:105802. doi:10.1016/j.enggeo.2020.105802
12. Abdollahipour A, Soltanian H, Pourmazaheri Y, Kazemzadeh E, and Fatehi-Marji M. Sensitivity Analysis of Geomechanical Parameters Affecting a Wellbore Stability. *J Cent South Univ* (2019) 26(3):768–78. doi:10.1007/s11771-019-4046-2
13. Ma T, and Chen P. A Wellbore Stability Analysis Model with Chemical-Mechanical Coupling for Shale Gas Reservoirs. *J Nat Gas Sci Eng* (2015) 26: 72–98. doi:10.1016/j.jngse.2015.05.028
14. Ding Y, Luo P, Liu X, and Liang L. Wellbore Stability Model for Horizontal wells in Shale Formations with Multiple Planes of Weakness. *J Nat Gas Sci Eng* (2018) 52:334–47. doi:10.1016/j.jngse.2018.01.029
15. Li X, Jaffal H, Feng Y, El Mohtar C, and Gray KE. Wellbore Breakouts: Mohr-Coulomb Plastic Rock Deformation, Fluid Seepage, and Time-dependent Mudcake Buildup. *J Nat Gas Sci Eng* (2018) 52:515–28. doi:10.1016/j.jngse.2018.02.006
16. Dokhani V, Yu M, and Bloys B. A Wellbore Stability Model for Shale Formations: Accounting for Strength Anisotropy and Fluid Induced Instability. *J Nat Gas Sci Eng* (2016) 32:174–84. doi:10.1016/j.jngse.2016.04.038
17. Li X, Yan X, and Kang Y. Investigation of Drill-In Fluids Damage and its Impact on Wellbore Stability in Longmaxi Shale Reservoir. *J Pet Sci Eng* (2017) 159:702–9. doi:10.1016/j.petrol.2017.10.005
18. Jia S, Xiao Z, Wu B, Wen C, and Jia L. Modelling of Time-dependent Wellbore Collapse in Hard Brittle Shale Formation under Underbalanced Drilling Condition[J]. *Geofluids* (2019) 2019:1–21. doi:10.1155/2019/1201958
19. Liang L, Xiong J, and Liu X. Experimental Study on Crack Propagation in Shale Formations Considering Hydration and Wettability. *J Nat Gas Sci Eng* (2015) 23:492–9. doi:10.1016/j.jngse.2015.02.032
20. Aadnoy BS. Stresses Around Horizontal Boreholes Drilled in Sedimentary Rocks. *J Pet Sci Eng* (1989) 2(4):349–60. doi:10.1016/0920-4105(89)90009-0
21. Zoback MD. *Reservoir geomechanics[M]*. Cambridge University Press (2010).
22. Deangeli C, and Omwanghe O. Prediction of Mud Pressures for the Stability of Wellbores Drilled in Transversely Isotropic Rocks. *Energies* (2018) 11(8):1944. doi:10.3390/en11081944
23. Setiawan NB, and Zimmerman RW. Wellbore Breakout Prediction in Transversely Isotropic Rocks Using True-Triaxial Failure Criteria. *Int J Rock Mech Mining Sci* (2018) 112:313–22. doi:10.1016/j.ijrmms.2018.10.033
24. Weijermars R, Wang J, and Nelson R. Stress Concentrations and Failure Modes in Horizontal wells Accounting for Elastic Anisotropy of Shale Formations. *Earth-Science Rev* (2020) 200:102957. doi:10.1016/j.earscirev.2019.102957
25. Singh A, Rao KS, and Ayothiraman R. An Analytical Solution to Wellbore Stability Using Mogi-Coulomb Failure Criterion. *J Rock Mech Geotechnical Eng* (2019) 11(6):1211–30. doi:10.1016/j.jrmge.2019.03.004
26. Li Y, and Weijermars R. Wellbore Stability Analysis in Transverse Isotropic Shales with Anisotropic Failure Criteria. *J Pet Sci Eng* (2019) 176:982–93. doi:10.1016/j.petrol.2019.01.092

Conflict of Interest: The authors declare that the research was conducted in the absence of any commercial or financial relationships that could be construed as a potential conflict of interest.

Publisher's Note: All claims expressed in this article are solely those of the authors and do not necessarily represent those of their affiliated organizations, or those of the publisher, the editors and the reviewers. Any product that may be evaluated in this article, or claim that may be made by its manufacturer, is not guaranteed or endorsed by the publisher.